3-3-3 Derivation of Near Real-time TEC for Monitoring Ionospheric Disturbances

MIYAKE Wataru and JIN Hidekatsu

We have developed a system of the rapid derivation of the total electron content (TEC) of the ionosphere from GEONET (a dense GPS receiver network in Japan), which offers unique opportunities for a permanent monitoring of the ionosphere. The latest TEC values (with a delay of 1–3 hours) are obtained every 3 hours, and most of the values are within 1–2 TEC units of the actual TEC. We have found the system quite powerful for continuously monitoring the progress of ionospheric storms. In addition to the plot of TEC temporal variation at 5 latitude regions over Japan, we have used a two-dimensional TEC map since 2008. The TEC map can detect the ionospheric disturbances over Japan, including large-amplitude traveling ionospheric disturbances, and plasma bubbles intruding over Japan, with high resolution. The development of the near realtime monitoring system of TEC enables us to monitor large ionospheric disturbances, ranging from global- to small-scale disturbances, expected in the next solar maximum. The plot and maps are open to the public and are available on http://wdc.nict.go.jp/IONO/.

Keywords
Total electron contents, Real-time monitoring, Ionospheric storms, Instrumental bias

1 Introduction

Variations in the space environment that could affect man-made spaces or ground mission-critical systems are called “space weather” by making an analogy to ground weather. One endeavor in progress aimed at alleviating the social effects of space weather is the research and development of a space weather prediction system (see [1]). In addition to developing a prediction algorithm, the readiness to gain quick insight into the current status of space weather forms an essential aspect of this prediction system, and, among other things, the task of expediting the process of collecting various observed values in real time and performing high-order data manipulations on those values assumes key importance.

One of the principal components of space weather is a variety of ionospheric disturbance phenomena that affect telecommunication, broadcasting and positioning performance. Developing ionospheric storms or solar flares are known to often disrupt communication in the HF band. Sporadic E-layer occurrences could cause even VHF signals to propagate anomalously, sparking interference with disaster-preparedness radio communications or TV broadcasts. Growing attention has also been focused in recent years on the impact of ionospheric disturbances on satellite positioning based on GPS satellites, etc. Higher total electron content (TEC) could cause delays in satellite-to-ground radio propagation and the disordered structure of electron density could result in scintillations.

This report introduces a system that derives the key ionospheric parameter of near real-time TEC, along with system implementation for monitoring ionospheric disturbances over Japan. Near real-time TEC derivation and monitoring systems have already been put to practical use and are made available to the general public in the U.S. and Europe

(see [2][3]). What is introduced here is Japan's first system of a similar kind developed by the National Institute of Information and Communications Technology on its own. The system offers features not found in the traditional scheme of ionosonde observation and rather complements it to provide a powerful solution for the task of monitoring ionospheric disturbances by means of near real-time TEC.

2 Deriving near real-time TEC

2.1 Derivation techniques

The velocity of radio propagation from a GPS satellite to the ground suffers a delay due to the ionospheric total electron content (TEC) encountered along the way. Because the delay is inversely proportional to the square of the frequency, the TEC value can be calculated from the propagation delay in a dual-frequency GPS-observed value. Each dual-frequency signal, however, has a different instrument delay bias that significantly affects TEC calculation accuracy. An estimation of instrumental biases should therefore be a prerequisite to deriving TEC. The instrumental biases consist of a satellite-specific satellite bias and a receiver-specific receiver bias.

Extensive research efforts have been directed worldwide to explore the techniques of estimating GPS satellite and receiver biases. In Japan, GPS receivers for the GPS Observation Network (GEONET) [4] inaugurated by the Geographical Survey Institute have been installed in many places nationwide. Otsuka et al [5]. estimated instrumental biases from data collected from these GPS receivers to derive the absolute values of TEC, thereby producing a two-dimensional TEC map with latitude/longitude resolutions of 0.15°×0.15°. Their technique, however, made no separation or distinction between satellite and receiver biases.

Ma and Maruyama [6], on the other hand, developed an algorithm for deriving TEC with these two kinds of biases separated by giving statistical manipulations to one day of GEONET data. It segmented the air above the entire country of Japan into 32 regions with latitude/longitude resolutions of 0.15°×0.15° as shown in Fig. 1, and assumed that the TEC value within each of these regions remains constant. Satellite and receiver biases were also assumed to remain constant within one day without variations. This algorithm was applied to GEONET data collected in 1997 and after to derive the TEC value every 15 minutes in each of the 32 regions, as well as day-to-day satellite and receiver biases, and then compile the data into a database. TEC data thus derived has been used in research on ionospheric storms, for example, in making many successful achievements (see Maruyama et al. [7]).

The algorithm developed by Ma and Maruyama [6] aimed at obtaining precise TEC values, but was not suited for deriving TEC in real time (because it required accumulating one day of GEONET data and involved a time-consuming computational process. Satellite and receiver biases vary with the lapse of time, but Ma and Maruyama [6] confirmed that such variations remain narrow, provided that the duration thereof did not exceed a few days.

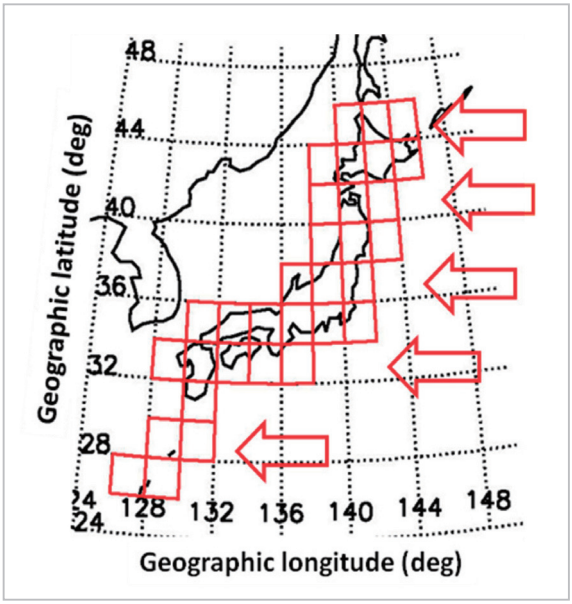

Fig. 1 *2°×2° meshes used to derive TEC and receiver/satellite biases*

Arrows point to the five latitude bands of 45°, 41°, 37°, 33°, and 29° used in the near real-time TEC plot.

Miyake [8] noted this fact and successfully speeded up the time needed to derive TEC by using biases in effect two to three days earlier. When all GPS and receiver biases are distinguished and known, then the TEC value can be easily derived for any satellite and receiver mix by solving the following equation:

$$TEC = (TECS - Br - Bs) \cos \chi \qquad (1)$$

where, TECS denotes the slant TEC over the path of radio propagation measured for the satellite-receiver pair, Br the receiver bias, Bs the satellite bias, and χ the satellite zenith angle. A prerequisite for deriving TEC from Equation (1) is that all values of Br and Bs are established. The method discussed here builds on the framework of deriving Br and Bs as implemented by the algorithm developed by Ma and Maruyama [6].

In the meantime, the preliminary values of GEONET data for the past six hours are now made available every three hours, as compared with one day of GEONET data released with a lag of two to three days before. Such preliminary values can be immediately corrected under ftp. Then, the bias values previously calculated from the data in effect several days earlier by implementing the algorithm developed by Ma and Maruyama [6] can be factored into the preliminary values to work out TEC in virtually real time. TEC can now be derived on a regular PC from GEONET data collected under ftp from the Geographical Survey Institute in processing time of up to 10 minutes.

2.2 Near real-time TEC error evaluation

The derived values of real-time TEC can be compared with the precise values of TEC calculated several days later by implementing the algorithm developed by Ma and Maruyama [6]. Figure 2 gives an example of such comparison. Four-day variations in TEC in the five latitude bands of 45°, 41°, 37°, 33° and 29° as shown in Fig. 1 are plotted from the top downward. TEC units ($\times 10^{16}$ electrons/ m^2)

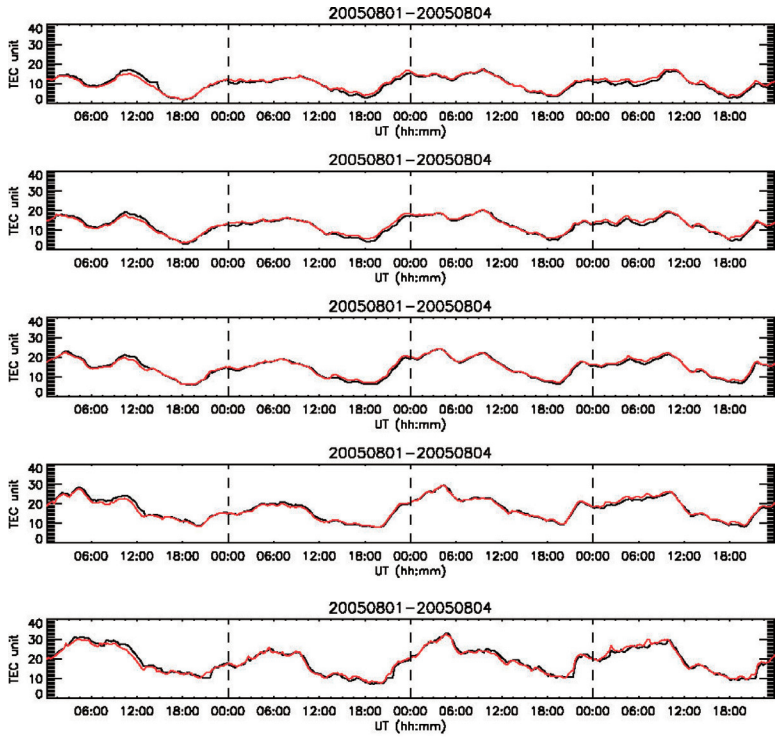

Fig.2 *Comparisons of TEC values derived in near real-time (red lines) with TEC values calculated later (black lines)*

Panels from the top downward denote the five latitude bands of 45°, 41°, 37°, 33°, and 29°.

are taken on the vertical axis, with the values of near real-time TEC marked along the red lines and the precise values of TEC calculated later along the black lines. Quiet-interval diurnal variations have been iterated over the four-day period without noticeable disturbances, when the value of near real-time TEC has moved without making much difference from its precise value, thereby attesting to the satisfactory accuracy of the monitoring system.

Figure 3 presents a statistical probe into the differences between the values of near real-time TEC over the latter six-month period of 2005 and the precise values of TEC calculated later. It concerns the frequency distributions of errors in the five latitude bands described earlier. Apparently, errors in near real-time TEC are confined to within ±1–2 TEC units in any latitude band. Here, the term "error" is defined as a near real-time TEC value less its precise value. According to root mean squares of the error distributions calculated, errors are found to equal 2.3, 1.6, 1.0, 1.2 and 1.7 TEC units from the highest latitude downward, and reaching minimum in the intermediate latitude band of 37°. One may jump at the conclusion that the receivers installed in this latitude band simply have narrow bias variations, but this is not necessarily true. Rather, it might be that the number of receivers included in each latitude band (2° × 2° region) has a greater effect on the errors.

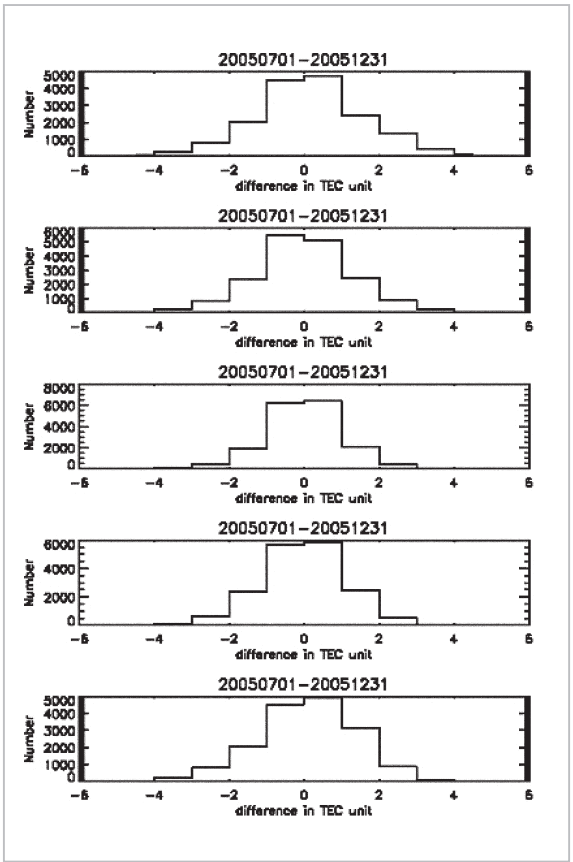

Fig.3 *Frequency distributions of differences between TEC values derived in near real-time in the five latitude bands over the latter six-month period of 2005 and the precise TEC values calculated later. Errors in near real-time TEC are basically confined to within 2 TEC units in any latitude band.*

The quantity of TEC data present in each latitude band varies momentarily as satellite positioning moves, but essentially depends on the number of receivers installed on the ground. The TEC values given in Figs. 2 and 3 are the averages calculated by dividing with the quantity of data at each point of time. Receiver biases are diverse; some turn positive in a matter of days while others become negative. As is evident from Equation (1), if receiver bias Br shifts to positive (or negative), then TEC proportionately posts a negative (or positive) error. If there is only one receiver to yield data in a given region, a receiver bias error would directly translate into a TEC error in that region. However, if a second receiver exists with a receiver bias error having the opposite sign, the effects of receiver bias errors in both receivers will be offset as the TEC values are averaged, resulting in the TEC error being narrowed. The greater the number of receivers, the closer the offset result is to 0. However, with fewer receivers, the offset may not work successfully (i.e., bias shift lopsided towards the same sign).

When the average quantity of data in each area is examined, each region of the 37° latitude band with the least error contained 33 units of data on the average in the periods shown in Fig. 3, as compared with 15 in each region of the 45° latitude band, or less than half the average quantity of data in each

region of the 37° latitude band. This reflects the number of receivers installed on the ground. On the central island of Honshu where a large number of receivers are located, TEC errors associated with the use of shifted bias values have been statistically narrowed. An examination of the correspondence between changes in the quantity of data in a given region caused by a moving satellite and TEC errors occasionally locates marked TEC errors with a reduced quantity of data.

3 Time-related changes in the TEC derivation system

The near real-time TEC derivation system has been commissioned into continuous service for ionospheric observatin purposes for four years to date since 2005. Time-related changes occurring in the system over this four-year period are summarized here. Figure 4 presents changes in the values of near real-time TEC and its precise values in the five latitude bands mentioned earlier. Root mean squares of the differences are plotted with regard to the first and second halves of each year under review. The differences are found to have virtually progressed within an error of 1 to 2 TEC units. By latitude, the size relationship between errors is the same for all periods, with errors being the largest in the latitude band of 45° and the smallest in the latitude band of 37°. As explained earlier, this finding should be taken for granted, provided that the size relationship between errors reflects the number of receivers installed in each latitude band. Moreover, errors were relatively large up until the first half of 2007, but diminished after the latter half of the year in all latitude bands. Something other than the receivers should be responsible for such simultaneous changes in all the latitude bands, because bias variations vary significantly from one receiver to another, rather than uniformly nationwide.

Figure 5 shows four-year variations in the satellite biases (continuous solid lines) and receiver biases (dashed lines), by plotting their root mean squares over a six-month period relative to all the satellites and all receivers installed nationwide. TEC units are taken on the vertical axis, with two-day and five-day variations marked in black and red lines, respectively. Both satellite and receiver biases are found to deviate by a wider margin with the lapse of time, with the red lines appearing larger than the black lines.

In the latter half of 2005 when the near real-time TEC derivation system had just been

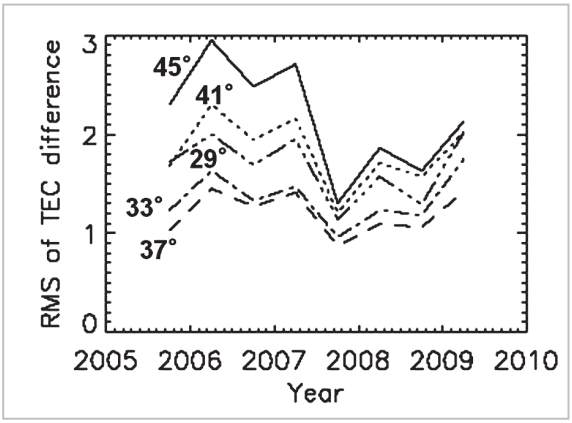

Fig.4 *Root mean squares of differences between TEC values derived in near real-time in the five latitude bands over a four-year period and the precise values of TEC calculated later. TEC units are taken on the vertical axis.*

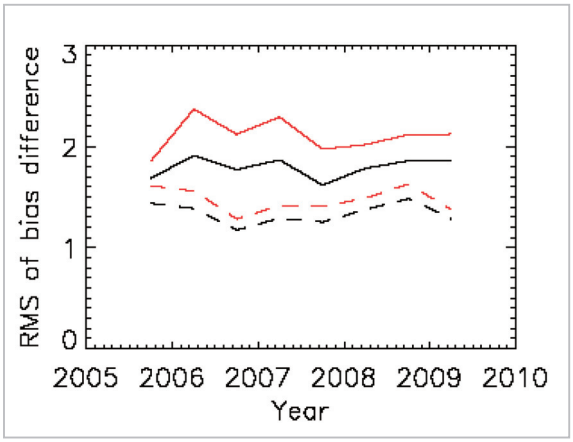

Fig.5 *Four-year changes in root mean squares of variations in satellite biases (continuous solid lines) and receiver biases (dashed lines)*

Two-day and five-day variations are marked in black and red lines, respectively. TEC units are taken on the vertical axis.

commissioned into service, the system would use bias values three days old in most cases or 4.8 days old on average due to a complication of various conditions, including unstable behavior of the GEONET server administered by the Geographical Survey Institute and the network installed on the premises of the National Institute of Information and Communications Technology, as well as the derivation system itself. These uncertainties had since been gradually diffused until the first half of 2007, when the currentness of bias values used on the derivation system improved to two days old in most cases and 3.0 days old on average. Therefore, the deviations of most biases should settle between the two colored lines in Fig. 5.

Comparing Fig. 4 with Fig. 5 will pinpoint similarities of the four-year changes in differences between the values of near real-time TEC and the precise values of TEC to the time-related changes in satellite (not receiver) bias variations equally in all latitude bands. As can be seen from Equation (1), each satellite bias deviation enters the data in all latitude bands equally as a constant error. Moreover, at least one and up to three satellites can be observed simultaneously, so that the effect of errors in individual satellite biases being offset by averaging a large quantity of observational data is not promising. This marks a sharp difference from errors resulting from receiver biases.

The near real-time TEC derivation system is characterized by its adoption of satellite and receiver biases recorded on different days to make real-time derivation possible. Information about errors in deriving TEC as a result of using biases from different days can be summarized as follows:

(1) Errors in near real-time TEC are basically confined to within 1 to 2 TEC units in any latitude band.
(2) Variations among individual receiver biases are diversified such that the effect of receiver bias variations will be offset by averaging in a region hosting a large number of receivers, such as the central island of Honshu, thereby exerting a limited effect on the values of real-time-TEC.
(3) In regions other than Honshu with fewer receivers, this offset has less effect and errors tend to appear more pronounced.
(4) No offset effect as described above extends to the effects of satellite biases, but their variations would directly translate into near real-time TEC errors. Time-related changes in the values of near real-time TEC reflect the amplitude of satellite bias variations.

4 Monitoring ionospheric disturbances

4.1 Ionospheric storms

Ionospheric modifications can be broken down into steady-state modifications, such as solar activity and seasonal and diurnal variations, and sudden modifications such as ionospheric storms following geomagnetic disturbances. To isolate and view spasmodic variations from the steady-state variation component, data for the past seven days is averaged at an equivalent time to work out average diurnal variations. Figure 6 presents data for the four days from December 12 to 15, 2006. In this diagram, the uppermost panel contains the Kp index that represents geomagnetic activity, with the five panels downward showing the values of near real-time TEC in the five latitude bands of 45˚, 41˚, 37˚, 33˚ and 29˚ as in Fig. 2. TEC units ($\times 10^{16}$ electrons/ m^2) are taken on the vertical axis, with average diurnal variations and observed values marked in black and red dashed lines, respectively. On the first to third days, the two lines are found to virtually overlap in every latitude band, demonstrating average diurnal variations without noticeable disturbances. On the fourth day, however, the observed values rise significantly above the averages in all latitude bands, providing evidence of sudden variations. A comparison with the Kp index suggests that an abnormal increase in TEC corresponds to acti-

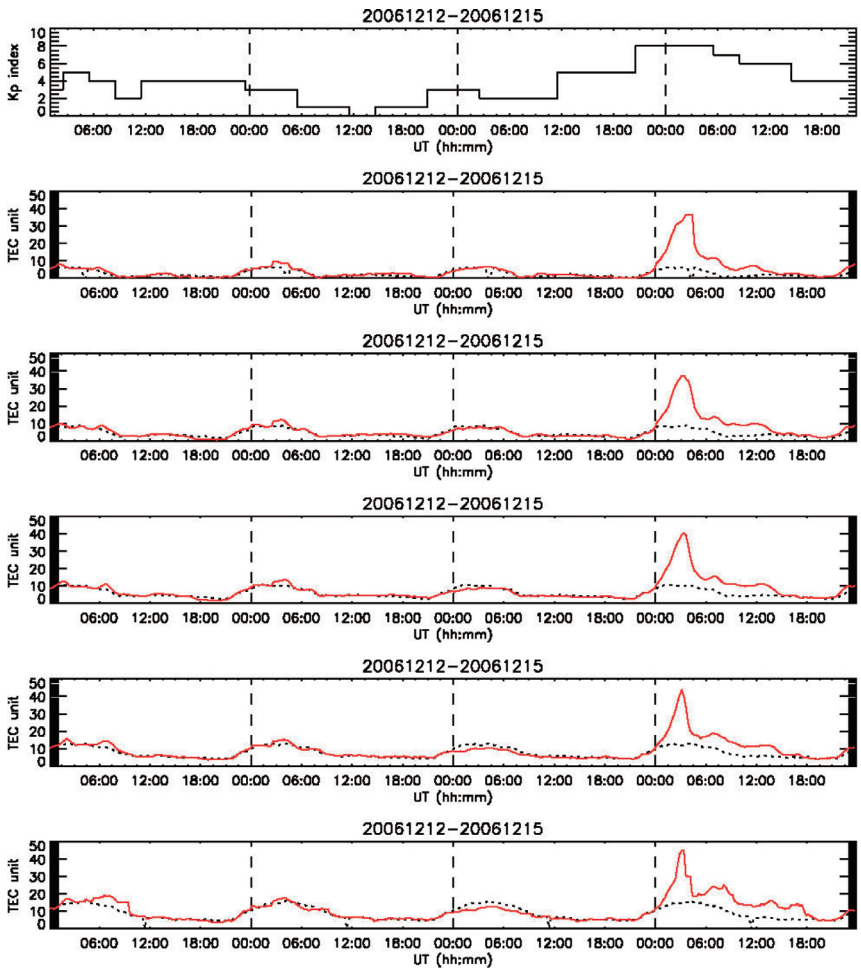

Fig.6 *Example of TEC variations in occurrence of positive ionospheric storms at geomagnetic disturbance time*

From the uppermost panel containing the Kp index downward, TEC variations in the five latitude bands over a four-day period are presented.

vated geomagnetic activity.

Ionospheric disturbances intensify energy input into the polar auroral zone, inducing massive modifications to the upper atmosphere (see [9][10]). If increases in molecular density (such as for N_2) extend to the mid- and low latitudes, its dissociative recombination with the primary F-region ions of O^+ is accelerated to reduce electron density in the ionosphere, resulting in negative ionospheric storms. The maximum usable frequency (MUF) in the HF band is then lowered to disrupt communications. In the meantime, if strong winds blow from the polar region toward the equator or the eastward electric field intensifies, the ionosphere is lifted up. As the altitude increases, molecules such as N_2 that extinguish O^+ are reduced in density to inhibit their dissociative recombination, resulting in higher electron density under sunshine conditions. This phenomenon is known as "positive ionospheric storms."

TEC—an integral value of electron density with respect to altitude—essentially varies as a direct parameter of changes in electron density of the F-region, which is higher than anywhere else. The increase in TEC that occurred on the fourth day as shown in Fig. 6 is an exact consequence of positive ionospheric storms. The Kp index had grown from the lat-

ter half of the third day, ushering in massive geomagnetic disturbances and resulting in an abnormal increase in ionospheric TEC under sunshine conditions. An example is not given here, but the occurrence of negative ionospheric storms can be monitored the same way with regard to deviations from the average diurnal variations identified in this plot of near real-time TEC. Some monitoring examples have been introduced by Miyake [8].

The ionospheric monitoring system based on near real-time TEC offers a number of benefits. Ionosonde observations had been used as a very effective means of observation long before commissioning of the near real-time TEC monitoring system. Their ionograms have offered extensive information about the ionosphere, including ionospheric critical frequency (foF2). Some weaknesses still remain, however. In Japan, the sporadic E-layer is frequently generated, mainly in summer time (see [11]). Where echoes from the F-layer are not obtainable with ionospheric storms occurring or developing, the present status is often not identifiable. In addition, echoes from the F-layer would also not be available in the presence of a shortwave fadeout (SWF) caused by X-ray flares. Interfaces from communication in the HF band could also hinder the work of reading echoes. Transmitter waves from GPS satellites have by far a higher frequency and render near real-time TEC harmless, allowing for full-time continuous monitoring of the ionospheric F-region.

Despite many years of research efforts made to date, whether positive or negative ionospheric storms occur in the wake of geomagnetic disturbances has yet to be precisely predicted. What we can now do is to monitor the occurrence and growth of ionospheric storms in real time and issue early warnings. In addition, occasional interchanges occurring between positive and negative ionospheric storms should be carefully and continuously monitored. From this viewpoint, real-time TEC is of great significance in that it has made the continuous monitoring of variations in the F-region associated with ionospheric storms possible, regardless of the concurrence or implication of other disturbance phenomena.

4.2 Examples of other disturbance phenomena

Aside from ionospheric storms, the real-time TEC monitoring system can identify such disturbance phenomena as equatorial anomalies, traveling ionospheric disturbances, and plasma bubbles. Figure 7 shows an example of equatorial anomalies developing into increased TEC over Japan's latitude bands. As shown in Fig. 6, the uppermost panel contains the Kp index and the five panels downward mark TEC variations in the five latitude bands in red continuous solid lines, with the average diurnal variations for the past seven days appearing in black dashed lines. As distinct from the case of ionospheric storms resulting from geomagnetic disturbances as shown in Fig. 6, the Kp index remains low for the four-day period while TEC exhibits an abnormal rise at the southernmost location of 29° on the fourth day, thereby illustrating the growth and penetration of equatorial anomalies into this latitude band.

Figures 6 and 7 give the average values of TEC falling into the same latitude band (2° width). The individual values are mapped in Figs. 8 and 9. Points are marked at the positions of projection at an ionospheric altitude of 350 km along the receiver-satellite line of sight and marked in different colors to designate the corresponding TEC values. Coordinates are the geographical latitude and longitude. Ionospheric storms and other phenomena that vary over a wide range simultaneously and are identifiable from deviations from their normal values would be easier to grasp when represented as shown in Fig. 6 or 7. Localized phenomena having a narrow spatial scale, however, should benefit from the two-dimensional mapping shown in Figs. 8 and 9. The GEONET receiver network is so densely deployed that it offers an excellent solution for detecting such localized phenomena. One such map is produced every five minutes to keep

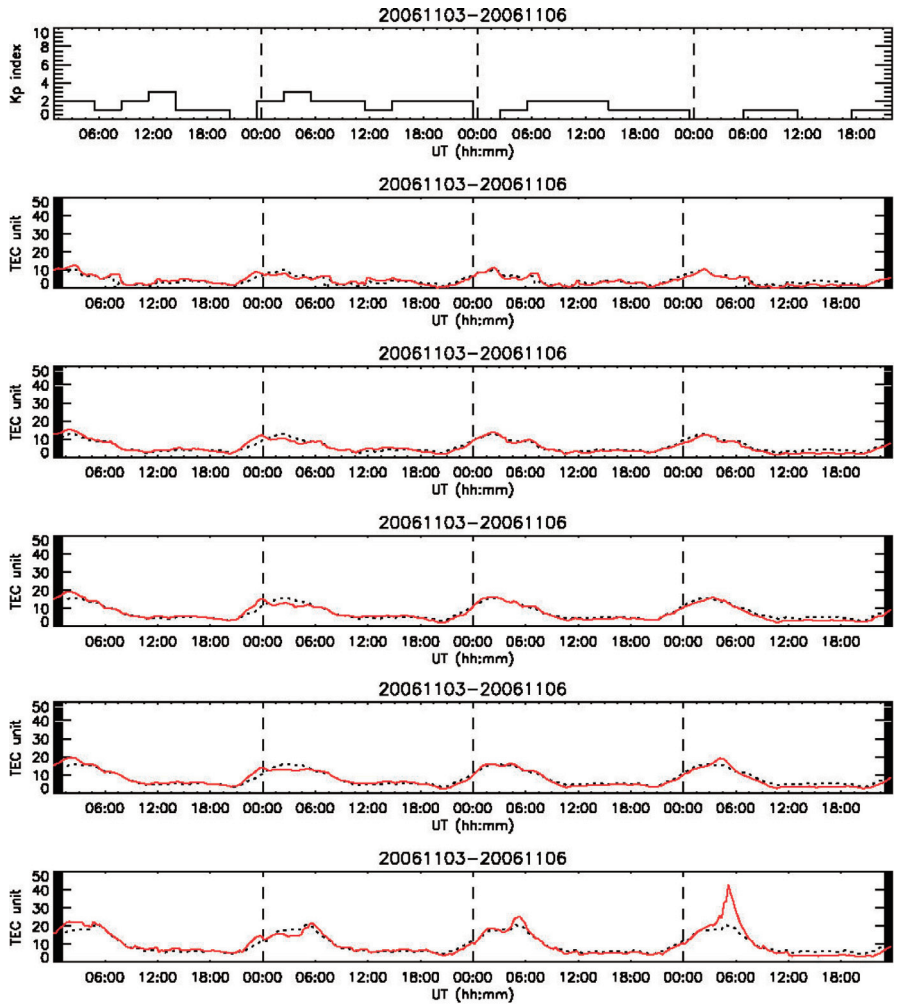

Fig.7 *Example of equatorial anomalies developing into increased TEC observed in the 29° latitude band of Japan (lowermost panel)*

From the uppermost panel containing the Kp index downward, TEC variations in the five latitude bands over a four-day period are presented.

detailed track of the time evolutions of phenomena. Since 2008, such maps have been added and made available to the general public, along with related animations. No noticeable abnormal phenomena have thus far occurred during the current period of solar activity minimum. Then, the scheme of mapping aided by this real-time TEC derivation system has been applied to the GEONET data in effect at the occurrence of abnormal phenomena during the preceding period of solar activity maximum to identify the kinds of phenomena that can be tracked down.

Figure 8 shows an example of traveling ionospheric disturbances (TID) (see [12]). A TEC structure with a wavefront exists in the northwest-southeast direction. A look at the preceding and succeeding times indicates that a wavelike structure had appeared around Hokkaido and propagated southwestward. Existing plots of TEC in the five latitude bands like those shown in Figs. 6 and 7 offer no insight into the wavelike structure or the status of radio propagation. The atmospheric expansion caused by the inflow and heating of pulsive energies into the polar region often induces propagated atmospheric disturbances (see [13]) toward the equator. Massive atmos-

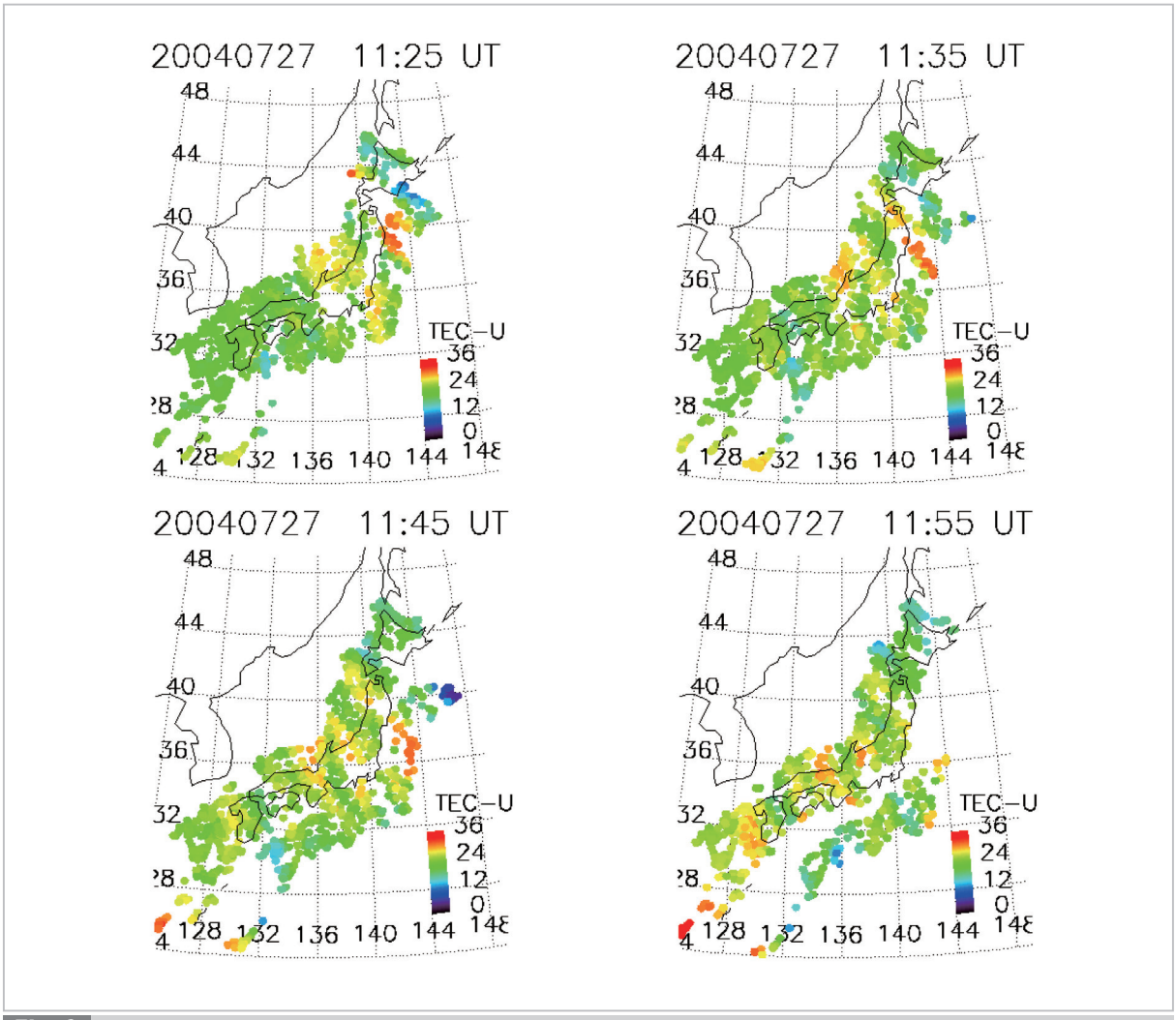

Fig.8 *Example of large-amplitude traveling ionospheric disturbances imparted southwestward over Japan*

Colors designate TEC values on a scale represented by the bar in the lower-right corner.

pheric gravitational waves are bound to be observed as increases or decreases in ionospheric, airglow intensity or TEC in the wavelike structure. The wavelike structure (called "medium-scale TID") has a wavelength of several hundreds of kilometers—an unusually large amplitude when compared with normal TID having a small amplitude not exceeding 1 TEC unit.

Plasma bubbles are structures of diminishing density formed in the equatorial region with a spatial gradient having high plasma density. Plasma bubbles grow in the lower part of the F-layer in a field-aligned current structure after sunset and ascend towards the upper ionosphere, reaching an altitude of 2000 km above the equator when the field-aligned current structure extends as far as Japan's latitude bands in certain situations [14][15]. A more detailed, irregular structure forms on the side of the plasma bubbles due to their density gradient, producing scintillations in signals transmitted from a satellite to the ground—one of the most serious sources of space environment disturbances (see [16]). Given this consideration, the National Institute of Information and Communications Technology is building an observation network in the Southeast Asian region in an effort to shed light on the mechanism of occurrence and propagation of plasma bubbles, thereby encouraging the development of prediction techniques [17].

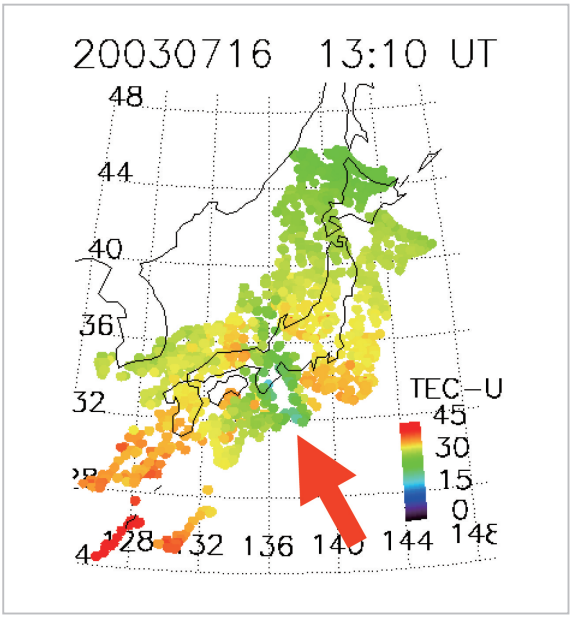

Fig.9 *Example of reductions in TEC associated with plasma bubbles forming above the land mass of Japan*

Figure 9 shows an example of a typical reduction in TEC resulting from plasma bubbles expanding above the land mass of Japan. TEC is found to have diminished in the region marked by the arrow. Ionosonde observatories are set up at four locations in Japan, and any plasma bubbles existing above these observatories should be detectable as they spread. In this phenomenon example, however, a plasma bubble positioned just between the two observatories in Kokubunji and Yamagawa is not caught by the ionosondes. Constant monitoring of such plasma bubbles expanding above Japan can be made possible through two-dimensional mapping of TEC based on the GEONET receiver network that seamlessly covers the entire land mass of Japan in high densities. A detailed discussion of typical ionospheric disturbance monitoring through a scheme of two-dimensional TEC mapping as reviewed here is reported by Miyake and Jin [18].

5 Conclusions

Ionospheric monitoring and prediction practices in the past largely targeted the occurrence of negative ionospheric storms, and were concerned with the disruption of communications caused by lowering of the maximum usable frequency (MUF) in the HF band. More recently, concern about the ionosphere has shifted to the impact of TEC on satellite navigation. The impact TEC may have on satellite navigation includes delays in radio propagation and lock-offs of satellite signals caused by ionospheric scintillations. The latter effect is liable to occur in the presence of a spatial gradient of intense TEC. A system is available to correct the location of a base station by deriving the amount of propagation delay from neighboring stations, but if a spatial gradient of intense TEC exists, base station correction information would end up involving a large error. Due to the declining importance of HF communication in social infrastructures, emphasis on the evolving course of ionospheric disturbance monitoring is expected to move towards disturbance phenomena having a large spatial gradient of TEC as depicted in Figs. 8 and 9. Gaining insight into the structures of such localized ionospheric disturbances should dictate their monitoring based on a two-dimensional map of real-time TEC to complement the work of ionosonde observations conducted at four locations nationwide.

Since the present real-time TEC monitoring system came into full-scale service, the solar activity minimum has set in, without significant ionospheric disturbances occurring. With the maximum of solar activity cycle 24 coming up around the corner, our monitoring system is expected to demonstrate its power in monitoring a variety of anticipated abnormal phenomena. Plots and two-dimensional maps of real-time TEC can be found at http://wdc.nict.go.jp/IONO/.

Acknowledgements

The authors wish to express their deep appreciation to Prof. Takashi Maruyama for his advice on implementing this research. Thanks are also due to Mr. Hisao Kato and

Ms. Itsuko Babasaki for their valuable assistance extended in our steady-state commissioning of this system and for the posting of plots on the Web.

References

1 Watari, S., "Impact of space storms on technologies and space weather forecast," J. Plasma Fusion Res., Vol. 82, No. 11, pp. 739–744, 2006.

2 Jakowski, N., S. M. Stankov, and D. Klaehn, "Operational space weather service for GNSS precise positioning," Ann. Geophysicae, Vol. 23, pp. 3071–3079, 2005.

3 Fuller-Rowell, T., E. Araujo-Pradere, C. Minter, M. Codrescu, P. Spencer, D. Robertson, and A. Jacobson, "US-TEC: A new data assimilation product from Space Environment Center characterizing the ionospheic total electron content using real-time GPS data," Radio Sci. Vol. 41, RS6003, doi: 10.1029/2005RS003393, 2006.

4 Miyazaki, S., T. Saito, M. Sasaki, Y. Hatanaka, and Y. Iimura, "Expansion of GSI's nationwide GPS array," Bulletin of the Geographical Survey Institute, Vol. 43, pp. 23–34, 1997.

5 Otsuka, Y., T. Ogawa, A. Saito T. Tsugawa, S. Fukao, and S. Miyazaki, "A new technique for mapping of total electron content using GPS network in Japan," Earth Planets Space, Vol. 54, pp. 63–70, 2002a.

6 Ma, G. and T. Maruyama, "Derivation of TEC and estimation of instrumental biases from GEONET in Japan," Ann. Geophysicae, Vol. 21, pp. 2083–2093, 2003.

7 Maruyama, T., G. Ma, and M. Nakamura, "Signature of TEC storm on 6 Novemver 2001 derived from dense GPS receiver network and ionosonde chain over Japan," J. Geophys. Res., Vol. 109, A10302, 2004.

8 Miyake, W., "Prompt derivation of TEC from GEONET data for space weather monitoring in Japan," J. Atmos. Sol-terr. Phys., Vol. 69, pp. 803–816, 2007.

9 Prölss, G. W., "Magnetic storm associated perturbations of the upper atmosphere," in Magnetic storms, Geophysical Monograph Ser., Vol. 98, pp. 227–241, 1997.

10 Buonsanto, M. J., "Ionospheric storms a review," Space Sci. Rev., Vol. 88, pp. 561–601, 1999.

11 Whitehead, J. D., "Recent work on mid-latitude and equatorial sporadic-E," J. Atmos. Terr. Physics, Vol. 51, pp. 401–424, 1989.

12 Saito, A. et al., "Traveling ionospheric disturbances detected in the FRONT campaign," Geophys. Res. Lett., Vol. 28, pp. 689–692, 2001.

13 Hocke, K. and K. Schlegel, "A review of atmospheric gravity waves and travelling ionospheric disturbances: 1982–1995," Ann. Geophysicae, Vol. 14, p. 917, 1996.

14 Otsuka, Y., K. Shiokawa, T. Ogawa, and P. Wilkinson, "Geomagnetic conjugate observations of equatorial airgrow depletions," Geophys. Res. Lett., Vol. 29, No. 15, pp. 1753–1756, 2002b.

15 Ogawa, T., E. Sagawa, Y. Otsuka, K. Shiokawa, T. I. Immel, S. B. Mende, and P. Wilkinson, "Simultaneous ground- and satellite-based airgrow observations of geomagnetic conjugate plasma bubbles in the equatorial anomaly," Earth Planets Space, Vol. 57, pp. 385–392, 2005.

16 Kelley, M., J. Makela, and O. de la Beaujardiere, "Convective ionospheric storms: a major space weather problem," Space Weather, Vol. 4, S02C04, doi: 10.1029/2005SW000145, 2006.

17 Maruyama, T., "Ionospheric irregularities," J. Commun. Res. Lab., Vol. 49, pp.163–179, 2002.

18 Miyake, W. and H. Jin, "Near-real time monitoring of TEC over Japan at NICT (RWC Tokyo of ISES)," Adv. Geosciences, Vol. 21, pp.143–153, 2010.

***MIYAKE Wataru**, Dr. Sci.*

Professor, School of Engeneering, Department of Aeronautics and Astronautics, Tokai University

Space Environment

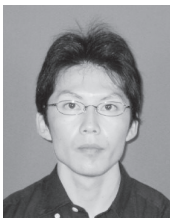

***JIN Hidekatsu**, Dr. Sci.*

Expert Researcher, Space Environment Group, Applied Electromagnetic Research Center

Upper Atmospheric Physics